

Final Program

2009 PHOTONICS CONFERENCE

December 2(Wed) ~ 4(Fri), 2009
Phoenix Resort, Pyeong Chang

Organized by

OSK / Photonics Division
KICS / Optical Communication Division
IEEK / Optical Wave and Quantum Electronics Division
KIEE / Optical Electronics and E.M. Wave Division
IEEE / PS Korea Chapter
SPIE / Korea Chapter

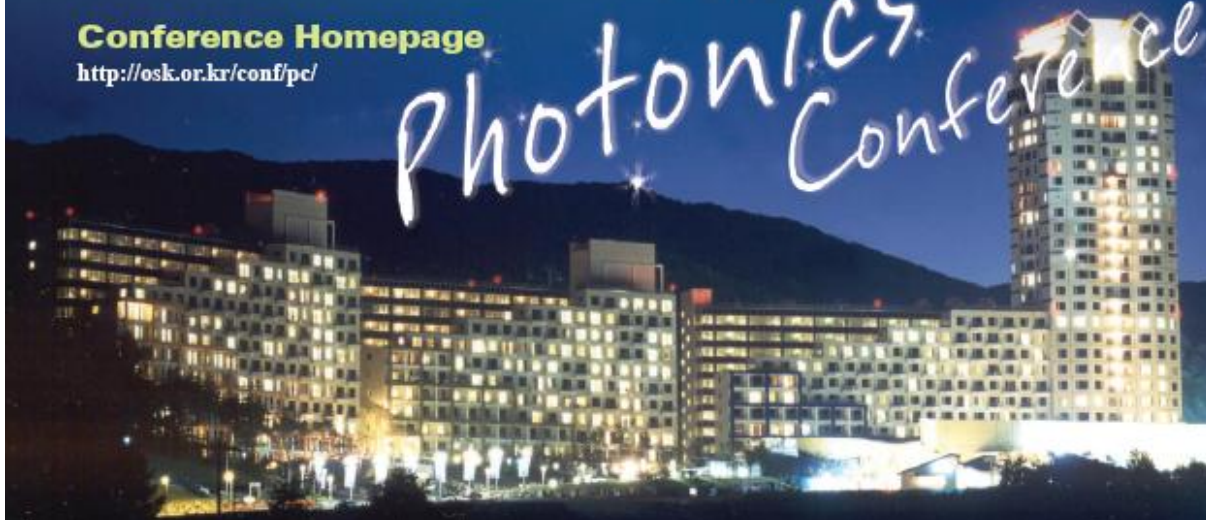
Sponsored by

KOFST / LUXPERT / ETRI / OPERA / HBL Corporation
LINKLINE Information&Communication
AlnoTech / Jinsan Micro-engineering Ltd
ChemOptics / OPHIT CO., LTD / KOPTI
WITHLIGHT / LiComm / SeongKyeong Photonics
EnerTeks / Kwang woon Univ. BK21
u&i Think Inc / KETI

Conference Homepage

<http://osk.or.kr/conf/pc/>

PHOTONICS
CONFERENCE



12월 2일 (수)

학술발표 W1A 다이아몬드 I
초고속광통신 I 14:00~15:30
좌장 : 장순혁(ETRI)

14:00(초정논문)
W1A-1 Coherent OFDM 신호의 IQ 불균형 보상과 분산 보상 없는 장거리 전송
정환석, 장순혁, 김광준(ETRI)
The performance enhancement using the Gram Schmidt orthogonal procedure for compensating IQ mismatch in coherent optical OFDM system are investigated. With IQ mismatch compensation, DCF-free transmission over 1040 km of conventional SMF is also presented.

14:30
W1A-2 56-Gbps 64-QAM 코히어런트 광 OFDM 링크에서의 I/Q 채널 위상 imbalance 수치 해석
홍문기, 권용욱, 김현승, 한상극(연세대), 권용환(ETRI)
I/Q channel phase imbalance effect on 56-Gbps 64-QAM coherent optical orthogonal frequency division multiplexed (OFDM) signal was analytically estimated by using the numerical model. As a result, we briefly estimated the validity of the transmission link of the certain data under the I/Q imbalance effect.

14:45
W1A-3 SCM 광 신호에서 광섬유의 분산과 SPM 현상의 영향에 대한 연구
김경수, 신재영, 안영빈, 이재훈, 정지채(고려대)
We studied the effect of fiber dispersion and self-phase modulation (SPM) on subcarrier multiplexed (SCM) optical signals. Numerical simulations based on the nonlinear Schrodinger equation were performed to calculate the detected RF subcarrier power after transmission over single-mode fiber (SMF) links. The results show that the combined effect of fiber dispersion and SPM can occur independently between subcarrier channels and the performance degradation is remarkable at the values of large OMI, small channel spacing, and large fiber launching power.

15:00
W1A-4 RSOA 를 사용한 25-GHz 채널간격의 128 채널 DWDM-PON
성창경, 이재승(광운대), 서경희(가톨릭대)
We demonstrate a dense WDM PON where 25-GHz spaced modulated in 10.7 Gb/s are distributed over a 15 km distance using 25-GHz and 200-GHz AWGs in series. For upstream signals, we use reflective SOAs.

15:15

학술발표 W1B 다이아몬드 II
광통신용소자 I 14:00~15:15
좌장 : 권용환(ETRI)

14:00(초정논문)
W1B-1 파장-잠김 F-P LD의 광세기 잡음 억제 기술
정종술(전 KAIST & LG-Nortel), 이창희(KAIST)
We propose optical noise suppression techniques for wavelength-locked Fabry-Perot laser diode (F-P LD) and demonstrate high capacity WDM-PON at 2.5 Gb/s. The noise suppressor located only at the central office enables smooth upgrade of deployed WDM-PON without modification of the outside plant.

14:30
W1B-2 WDM-PON에서 컬러리스 가미자 광편을 위한 2.5Gbps RSOA 제작 및 특성
김동철, 최영석, 김현수, 김기수, 박미란, 권오근, 오대근(ETRI)
In this paper, we present fabrication and device/packaged-module characteristics of RSOA for WDM-PON ONU. Optical gain, 3dB ASE bandwidth and polarization dependent gain were about 25 dB, 35 nm and less than 1.0 dB, respectively. At 2.5 Gbps, ROSA shows clear eye-diagram. After 2.5 Gbps-20 km transmission, BER shows error free operation and power penalty was about 1.9 dB at 10⁻⁹ BER.

14:45
W1B-4 C-band 반도체 광증폭기 모듈 제작 및 특성
이동훈, 심은덕, 이철축, 김종희, 권오기, 김영안, 백용순(ETRI)
This paper reports on the fabrication and characteristics of C-band Semiconductor optical amplifier (SOA) modules with various optical confinement factors of Active layer. Tensile-strained InGaAsP Bulk Active was used for low polarization-independent gain and ridge-based spot-size converters (SSC) were integrated on both side of SOA.

15:00
W1B-5 표준 CMOS 공정에서 Geiger-Mode Avalanche Photodiode 을 고속 동작시키기 위한 주변 회로
권인용, 이영재, 성창경, 윤진성, 최우영(연세대)
An active quench and reset circuit (AQRC) in peripheral circuits makes G-APD to detect weak optical signals in high speed by reducing dead time. We performed the post-layout simulation of proposed AQRC with 0.13-um standard CMOS technology. With the proposed AQRC scheme, the dead time is decreased to 7 ns.

학술발표 W1C 에메랄드
광섬유레이저 14:00~15:30
좌장 : 오경환(연세대)

14:00(초정논문)
W1C-1 아토초-정밀도 초고속 광섬유 광학
김정원(KAIST)
I review the recent progress toward the attosecond-precision ultrafast optics using fiber optic techniques. The concentration of large number of photons in an extremely short pulse duration enables the scaling of timing jitter of femtosecond mode-locked lasers into the attosecond regime. Further, the unique property of optical pulse trains of simultaneously carrying ultralow-jitter optical and microwave/RF signals enables unprecedented timing precision in both optical and electronic domains. In this presentation, an array of new ultrafast optic techniques for the synthesis, distribution and characterization of ultralow-jitter optical and microwave/RF signals is presented.

14:30
W1C-2 졸겔 글라스에 균일 분산된 탄소나노튜브를 이용한 초고속 광섬유 펄스 레이저
한원석, 배미경, 송용현(KIST)
We prepare carbon nanotube (CNT)-incorporated sol-gel glass at low temperature guaranteeing homogeneous CNT dispersion in the host as well as the intact nonlinearity of CNTs for an all-fiber laser mode-locker. The fabricated passively mode-locked laser has the pulsed output with the spectral bandwidth of 1.1 nm and the repetition rate of 2.96 MHz.

14:45
W1C-3 고효율 Yb3+ 도핑 광섬유 증폭기에 있어서 입력 펄스 파형의 특성 분석
이준수, 이주한(서울시립대)
Based on numerical modeling, the dynamic waveform of high-power ytterbium-doped double-clad fiber amplifier during the amplification of nanosecond is analyzed.

15:00
W1C-4 그래핀을 이용한 고효율 광섬유 펄스 레이저
배미경, 한원석, 장성연, 송용현(KIST)
We demonstrate a fiber pulsed laser passively mode-locked by Graphen in high-power regime. In order to circumvent the thermal damage of the nanostructure, we successfully realize an evanescent field interaction of the propagating light with graphene layer to form picosecond pulses.



High-Speed Peripheral Circuit for Geiger-Mode Avalanche Photodiode in Standard CMOS Technology

Inyong Kwon*, Myung-Jae Lee, Chang-Kyung Seong, Jin-Sung Youn, and Woo-Young Choi
Department of Electrical and Electronic Engineering, Yonsei University, Korea
E-mail: wchoi@yonsei.ac.kr

Abstract An active quench and reset circuit (AQRC) in peripheral circuits makes G-APD to detect weak optical signals in high speed by reducing dead time. We performed the post-layout simulation of proposed AQRC with 0.13- μm standard CMOS technology. With the proposed AQRC scheme, the dead time is decreased to 7 ns.

I. INTRODUCTION

Photon counting via single photon detection is the technique of choice when measuring low level optical signals. The intensity of this signal is determined by the number of photons detected in a given time [1]. Then detecting photons is important in low intensity light applications such as defect monitoring of CMOS processes and circuits, optical time domain reflectometry (OTDR), laser ranging, fluorescence lifetime measurement, fluorescence spectroscopy and astronomy. For the purpose of photon counting, the avalanche photodiode (APD) is biased above its breakdown voltage in Geiger mode and is often referred to as a Geiger-mode APD (G-APD) or single photon avalanche diode (SPAD). When an avalanche breakdown occurs in depletion region, macroscopic current flows through the G-APD. In order to limit this current, a resistor is included in series with the G-APD. This simple resistor allows passive quenching [2] of the avalanche current and resets the bias on the detector once the avalanche current falls to zero. The main disadvantage of this circuit is that the quiescent voltage bias is recharged through the high value quench-resistor and the diode depletion capacitance giving a long reset time, typically in the microsecond range. This leads to a long dead time between detected photons. In this paper, to overcome the limitations posed by passive quenching and to optimize the performance of a G-APD in high-speed photon counting, an active quench and reset circuit (AQRC) is used. The AQRC circuit reduced the dead time in 7ns and is a remarkable output rather than the previously reported results.

II. ACTIVE QUENCH AND RESET CIRCUIT

The proposed AQRC is designed with standard 0.13- μm CMOS technology and is based on a passive AQRC by Zappa et al [3]. For precise simulation, G-APD is simply modeled by characteristics which are a 500 fC parasitic capacitor and a 100 μA current source of APD studied by Myung-Jae Lee et al [4]. As an electron-hole pair is generated in the depletion region of the G-APD, either by an incident photon or thermal generation, avalanche process is started. This avalanche current builds up, and the AQRC set in motion.

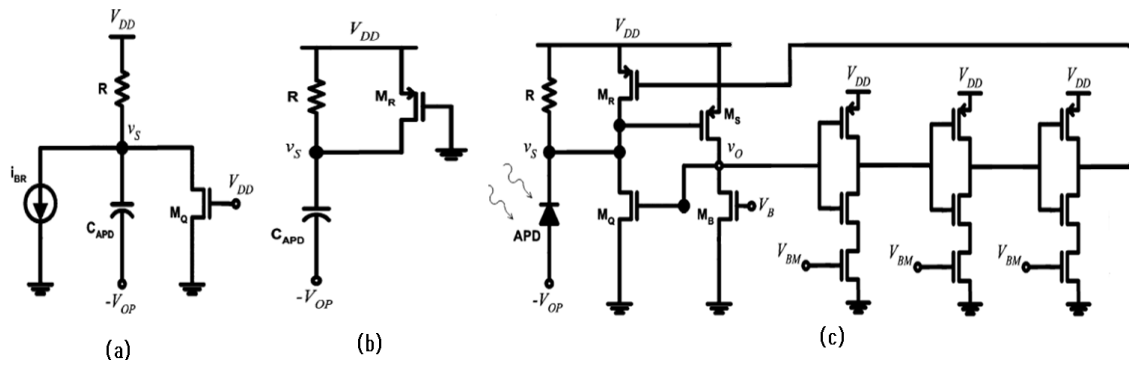


Fig. 1. Equivalent circuits of the sense node v_s (a) during active quench and (b) active reset. (c) Schematic of the G-APD with active quench and active reset.

In Fig. 1 (a) and (b) are quench and reset circuit, respectively. Fig. 1 (c) is the whole schematic with active quench, active reset, and delay circuits which are consisted of three inverters and control transistors. Although operating process of the quench and reset circuit is based on [5], the delay circuit has a different structure. The delay circuit is very simplified by using only three inverters that the delay can be controlled by bias voltages V_{BM} . Whereas complicated delay circuit involved with a capacitor is used to find out an end point of incident photons to G-APD as a falling edge detector, the delay circuit on this work is operated immediately and automatically when photon is incident to G-APD.

III. SIMULATION RESULTS AND CONCLUSION

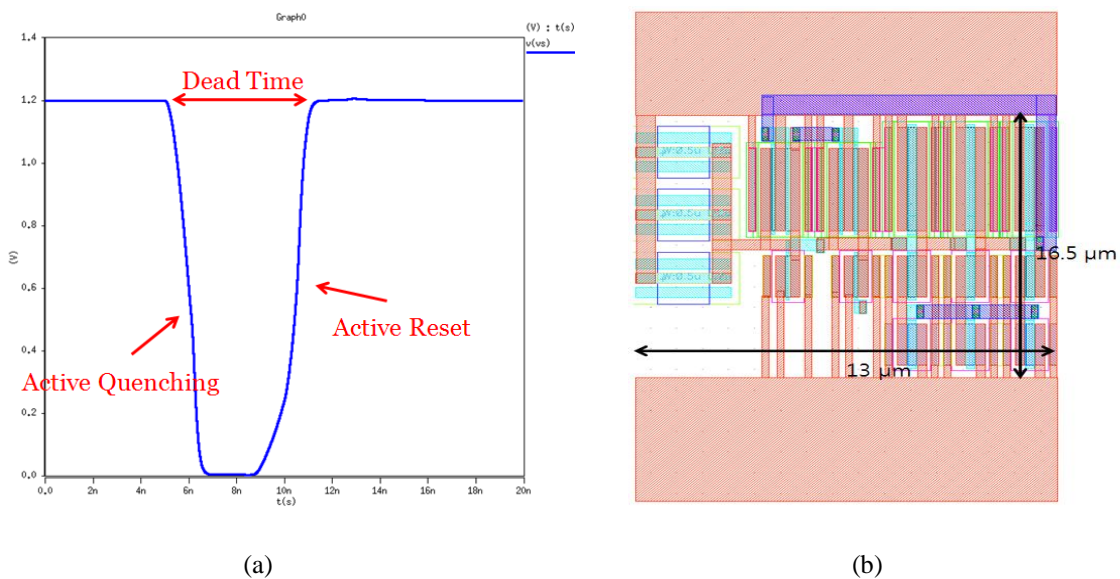


Fig. 2. (a) Post-layout simulated sense node v_s voltage of the whole circuit. The dead time is 7ns. (b) Whole layout consisted of quench, reset, and delay circuit

Fig. 2 (a) shows the post-layout simulation results of the proposed peripheral circuits. With our peripheral circuits, quench and reset times are significantly reduced which achieves dead-time of 7 ns. Since the start of avalanche in the G-APD, v_S will start to drop with passive quenching. Fig. 2 (a) shows a quench time of about 2 ns and a reset time of about 2 ns. This simple AQRC reduced dead time into 7 ns and required small area $13 \mu\text{m}$ by $16.5 \mu\text{m}$ as shown in Fig. 2 (b), whereas previous results of G-APDs with CMOS technology have reported dead times of 60 ns [6], 40 ns [7], and 13 ns [4].

REFERENCE

- [1] Stephen B. Alexander, *Optical Communications Receiver Design*, SPIE, IEEE, 1997.
- [2] Cova S., et al., "Active-quenching and gating circuits for single-photon avalanche diodes (SPADs)," *IEEE Trans. Nucl. Sci.*, no. 29, pp. 599–601, October 1981.
- [3] Zappa F., et al., "Monolithic Active-Quenching and Active-Reset Circuit for Single-Photon Avalanche Detectors", *IEEE J. Solid-State Circuits*, vol. 38, no. 7, pp. 1298–1301, Jul. 2003.
- [4] M. J. Lee, et al., "Equivalent circuit model for Si avalanche photodetectors fabricated in standard CMOS process", *IEEE Electron Devices Lett.*, vol. 90, no. 15, pp. 151118-1–151118-3, Apr. 2007.
- [5] Faramarzpour. N, et al., "Fully Integrated Single Photon Avalanche Diode Detector in Standard CMOS 0.18- μm Technology", *IEEE Trans. Electron Devices*, vol. 55, no. 3, pp. 760-767, 2008.
- [6] Tisa S., et al., "On-chip detection and counting of single-photons," *IEEE Photon. Technol. Lett.*, vol. 17, no. 1, pp. 184-186, Jan. 2005.
- [7] Niclass C., et al., "Design and Characterization of a CMOS 3-D Image Sensor Based on Single Photon Avalanche Diodes", *IEEE J. Solid-State Circuits*, vol. 40, no. 9, pp. 1847–1854, Sep. 2005.